Potential Neuroprotective Effects of an LSD1 Inhibitor in Retinal Ganglion Cells via p38 MAPK Activity

Takayuki Tsutsumi,[1] Keiichiro Iwao,[1] Hideki Hayashi,[2] Tomoko Kirihara,[3] Takahiro Kawaji,[1] Toshihiro Inoue,[1] Shinjiro Hino,[4] Mitsuyoshi Nakao,[4] and Hidenobu Tanihara[1]

[1]Department of Ophthalmology and Visual Science, Kumamoto University Graduate School of Medical Sciences, Kumamoto, Japan
[2]Department of Applied Biochemistry, School of Pharmacy, Tokyo University of Pharmacy and Life Sciences, Tokyo, Japan
[3]Translational Science, R&D Division, Santen Pharmaceutical Co., Ltd., Osaka, Japan
[4]Department of Medical Cell Biology, Institute of Molecular Embryology and Genetics, Kumamoto University, Kumamoto, Japan

Correspondence: Keiichiro Iwao, Department of Ophthalmology and Visual Science, Kumamoto University Graduate School of Medical Sciences, 1-1-1 Honjo, Kumamoto 860-8556, Japan; iwaokei@fc.kuh.kumamoto-u.ac.jp.

Submitted: March 4, 2016
Accepted: October 26, 2016

Citation: Tsutsumi T, Iwao K, Hayashi H, et al. Potential neuroprotective effects of an LSD1 inhibitor in retinal ganglion cells via p38 MAPK activity. *Invest Ophthalmol Vis Sci*. 2016;57:6461–6473. DOI:10.1167/iovs.16-19494

Purpose. The epigenetic mechanisms associated with ocular neurodegenerative diseases remain unclear. The present study aimed to determine the role of lysine-specific demethylase 1 (LSD1), which represses transcription by removing the methyl group from methylated lysine 4 of histone H3, in retinal ganglion cell (RGC) survival, and to investigate the details of the neuroprotective mechanism of tranylcypromine, a major LSD1 inhibitor.

Methods. The authors evaluated whether tranylcypromine contributes to neuronal survival following stress-induced damage using primary cultured rat RGCs and in vivo N-methyl-D-aspartate (NMDA)-induced excitotoxicity. Additionally, the molecules associated with tranylcypromine treatment were assessed by microarray and immunoblot analysis.

Results. Tranylcypromine significantly suppressed neuronal cell death following glutamate neurotoxicity and oxidative stress. Microarray and immunoblot analyses revealed that p38 mitogen-activated protein kinase (MAPK)γ was a key molecule involved in the neuroprotective mechanisms induced by tranylcypromine because the significant suppression of p38 MAPKγ by glutamate was reversed by tranylcypromine. Moreover, although pharmacologic inhibition of the phosphorylation of the total p38 MAPKs interfered with neuroprotective effects of tranylcypromine, the specific inhibition of p38 MAPKα and p38 MAPKβ did not influence RGC survival. This suggests that the non-p38 MAPKα/β isoforms have important roles in neuronal survival by tranylcypromine. Additionally, the intravitreal administration of tranylcypromine significantly saved RGC numbers in an in vivo glaucoma model employing NMDA-induced excitotoxicity.

Conclusions. These findings indicate that tranylcypromine-induced transcriptional and epigenetic regulation modulated RGC survival via the promotion of p38 MAPKγ activity. Therefore, pharmacologic treatments that suppress LSD1 activity may be a novel therapeutic strategy that can be used to treat neurodegenerative diseases.

Keywords: tranylcypromine, neuroprotection, survival, glaucoma, epigenetic drug

Glaucoma is a major optic neuropathy characterized by the significant loss of retinal ganglion cells (RGCs)[1] and is a leading cause of blindness around the world.[2–4] Retinal ganglion cell death directly causes visual field deficits, and the primary risk factor associated with progressive damage to the visual field is elevated intraocular pressure (IOP).[5–7] However, RGCs may suffer damage even in normal-tension glaucoma patients in which IOP is within the normal range (10–21 mm Hg).[8]

Recent epidemiologic studies have demonstrated that normal-tension glaucoma is more common than high-tension glaucoma among primary open-angle glaucoma patients, particularly in Asian populations.[9–12] The causes of normal-tension glaucoma have yet to be completely elucidated; however, a variety of factors, including reduced blood flow in the optic nerve,[13] genetic variables,[14,15] and an enlarged gap between cerebrospinal fluid pressure and IOP,[16] may be involved in the pathophysiology of this disease. Evidence-based treatments for patients with glaucoma, including normal-tension patients, target reductions in IOP via ophthalmic solutions, laser therapy, or surgery.[17] However, the therapeutic efficacies of these treatments are often limited and may be clinically insufficient even though they lower IOP. Thus, novel treatment strategies for glaucoma, such as the neuroprotection of RGCs, are urgently required.

Except for alterations in the original DNA sequence via DNA methylation, the modulation of histone, or noncoding RNA, epigenetic changes influence gene expression and function.[18] It is well known that histone is specifically modified by a variety of mechanisms, including the acetylation of histone N-terminal tails, methylation, phosphorylation, ubiquitination, and adenosine diphosphate (ADP) ribosylation.[19] Histone modification involves switches that alter chromatin structure or form binding platforms that allow for downstream effector proteins to induce transcriptional activation or repression.[20]

Several recent reports have suggested that multiple epigenetic factors play important roles in the survival and pathogenesis of RGCs in models of glaucoma. For example,

damage to RGCs via crushing of the optic nerve leads to changes in the activity of histone deacetylases (HDACs), which are a key factor in the deacetylation of histone.[21] However, these authors also reported that the inhibition of retinal HDAC activity by trichostatin A preserved the expression of representative RGC-specific genes and attenuated cell loss following optic nerve damage. Valproic acid, which is another popular HDAC inhibitor, also exerts neuroprotective effects and induces axonal regeneration following optic nerve crushing via regulation of the transcription factor cyclic adenosine monophosphate (cAMP) response element binding protein (CREB).[22] Additionally, valproic acid prevents RGC death in N-methyl-D-aspartate (NMDA)-induced glaucoma model and GLAST-knockout glaucoma model mice, via stimulation of neuronal TrkB receptor signaling.[23,24] Furthermore, the genetic ablation of *Hdac3* in RGCs results in a significant amelioration of nuclear atrophy as well as significant suppression of cell death during the acute phase after optic nerve injury.[21,25] These findings imply that the transcriptional downregulation and initiation of cell death mechanisms in neurodegenerative diseases, including glaucoma, may be linked with epigenetic processes.

Recent investigations of the relationship between histone acetylation/deacetylation and neuronal survival have revealed that HDAC inhibitors exert neuroprotective effects against neurodegeneration.[21–25] However, the role that histone methylation plays in ocular neurodegenerative diseases, including glaucoma, remains unclear. Thus, the present study aimed to investigate the relationship between histone methylation and the function of lysine-specific demethylase 1 (LSD1), which demethylates histone H3 at lysine 4 (H3K4) or H3K9 via a flavin-dependent oxidation reaction and induces transcriptional repression in general[26,27] during neuronal survival and neurodegeneration in glaucoma. The present findings demonstrated the importance of LSD1 activity in RGC survival as well as the neuroprotective effects of tranylcypromine, which is a major LSD1 inhibitor. Furthermore, this study identified and clarified possible molecular targets involved in the tranylcypromine-mediated protection of RGCs. Taken together, these findings suggest that LSD1 is a key regulator of neuronal cell survival and a potential molecular target for the treatment of neurodegenerative diseases.

Methods

Reagents and Animals

The present study utilized tranylcypromine, which is also known as 2-phenylcyclopropylamine hydrochloride (Sigma-Aldrich Corp., St Louis, MO, USA), and S2101, which is also known as LSD1 Inhibitor II (no. 489477; Merck Millipore, Billerica, MA, USA). The isolation of RGCs was performed using 2-day-old Sprague-Dawley (SD) rats (Kyudo Co., Ltd., Kumamoto, Japan), and 8-week-old male Slc:SD rats (Japan SLC, Inc., Shizuoka, Japan) were used for optic nerve crush experiments. All experimental procedures were performed in accordance with the ARVO Statement for the Use of Animals in Ophthalmic and Vision Research, and all experimental procedures were approved by the Animal Care Committee of Kumamoto University.

Primary Cultures of RGCs

Primary cultured RGCs were purified using a two-step immunopanning method, as previously described,[28] with minor modifications.[29–31] Briefly, the retinas were digested with papain (16.5 units/mL) and triturated with rabbit anti-rat macrophage antiserum (Accurate Chemical, Westbury, NY, USA). The cell suspension was first incubated on a panning plate (150-mm petri dish; BD Falcon, Franklin Lakes, NJ , USA) coated with goat anti-rabbit IgG (Thermo Fisher Scientific, Waltham, MA, USA). The nonadherent cells were incubated on a second panning plate (100-mm petri dish; Thermo Fisher Scientific) coated with goat anti-mouse IgMμ (Thermo Fisher Scientific) and mouse anti-Thy1.1 antibodies secreted from T11D7e2 cells (American Type Culture Collection, Manassas, VA, USA). Next, the plate was washed with phosphate-buffered saline (PBS), and the adherent RGCs were released by treatment with 0.125% trypsin (Sigma-Aldrich Corp.).

The isolated RGCs were suspended in a medium containing 1 mM glutamine, 5 μg/mL insulin, 60 μg/mL *N*-acetylcysteine, 62 ng/mL progesterone, 16 μg/mL putrescine, 40 ng/mL sodium selenite, 0.1 mg/mL bovine serum albumin (BSA), 40 ng/mL triiodothyronine, 0.1 mg/mL transferrin, 1 mM sodium pyruvate, 2% B27 supplement (no. 17504-044; Invitrogen, Carlsbad, CA, USA), 10 μM forskolin, 50 ng/mL brain-derived neurotrophic factor (BDNF; PeproTech, Rocky Hill, NJ, USA), 50 ng/mL ciliary neurotrophic factor (CNTF; PeproTech), and 50 ng/mL basic fibroblast growth factor (bFGF; PeproTech) in Neurobasal medium (Thermo Fisher Scientific). Finally, 96-well culture plates were coated with poly-D-lysine (Sigma-Aldrich Corp.) and laminin (Sigma-Aldrich Corp.), and the RGCs were plated at a density of 5000 cells/well and cultured for at least 10 days prior to the experimental procedures.

Immunoblotting

The immunoblotting procedures were performed as previously described.[29–31] Briefly, the proteins were separated using sodium dodecyl sulfate polyacrylamide gel electrophoresis (SDS-PAGE), transferred to polyvinylidene difluoride (PVDF) membranes, and probed with primary and peroxidase-conjugated secondary antibodies. The immunoreactive proteins were visualized with SuperSignal West Pico, Dura, or Femto (Thermo Fisher Scientific) using the following primary antibodies: mouse anti-β-actin (no. A5441; Sigma-Aldrich Corp.), rabbit anti-LSD1 (C69G12, no. 2184; Cell Signaling Technology, Danvers, MA, USA), rabbit anti-phosoho-p38MAPK ([Thr180/Tyr182][D3F9], no. 4511; Cell Signaling Technology), rabbit anti-p38MAPK (no. 9212; Cell Signaling Technology), rabbit anti-p38 MAPKγ (no. 2307; Cell Signaling Technology), rabbit anti-phospho-Akt (Ser473, no. 9271; Cell Signaling Technology), rabbit anti-Akt (no. 9272; Cell Signaling Technology), and rabbit anti-cleaved caspase 3 (Asp175, no. 9661; Cell Signaling Technology).

Apoptosis of RGCs

The evaluation of RGC apoptosis was performed as previously described.[31] Briefly, the primary cultured RGCs were washed twice (15-minute incubation at 37°C) with Hanks' balanced salt solution (HBSS; Invitrogen) containing 2.4 mM $CaCl_2$ and 20 mM HEPES without magnesium; the magnesium was omitted from the washing solution to avoid blocking the NMDA receptor.[32] Subsequently, the RGCs were incubated in 300 μM glutamate and 10 μM glycine, which is a coactivator of the NMDA receptor, in HBSS containing 2.4 mM $CaCl_2$ and 20 mM HEPES without magnesium for 2 hours at 37°C. After treatment with glutamate, the RGCs were cultured in the same medium without any neurotrophic factors such as forskolin, BDNF, CNTF, or bFGF for 22 hours at 37°C. Oxidative stress–induced cell death was achieved by the addition of 50 μM hydrogen peroxide (H_2O_2) with trophic additives containing B27 supplement AO depleted of antioxidants (Invitrogen) for 30 minutes and then incubating the cells for 24 hours. Tranylcy-

promine (100 μM) and wortmannin (100 nM, no. 681675; Merck Millipore) were simultaneously administered with the glutamate or H_2O_2, while S2101, BIRB796 (10 μM, no. S1574; Selleck Chemicals, Houston, TX, USA), and SB203580 (10 μM, no. 199-16551; Wako, Osaka, Japan) were added 24 hours before the induction of apoptosis. Subsequently, the treated RGCs were incubated for 24 hours prior to the detection of apoptosis.

Apoptosis was detected by incubating the RGCs with 1.0 μg/mL Hoechst 33342 (Dojindo, Kumamoto, Japan) for 15 minutes. The fluorescent images were observed using an IX71 fluorescence microscope (Olympus, Tokyo, Japan), and at least six images/well were obtained from the 96-well plates. As previously described,[30,31] the fragmented or shrunken nuclei stained with Hoechst dye were counted as apoptotic neurons and the round/smooth nuclei were considered to be healthy neurons. For each condition, more than 200 neurons were counted using MetaMorph imaging software (Molecular Devices, Sunnyvale, CA, USA) to minimize measurement biases.

Lsd1 RNA Silencing

Either nonsilencing small interfering RNA (siRNA; 1 μM Accell nontargeting siRNA no. 1; Thermo Fisher Scientific) or *Lsd1*-specific siRNA (E-105863-00-0010; Accell Rat *Kdm1a* [Gene ID: 500569] siRNA SMARTpool; Thermo Fisher Scientific) was added to the culture medium according to the manufacturer's instructions and then incubated with the RGCs for 6 days. The knockdown effect of the *Lsd1*-specific siRNA was confirmed using an immunoblotting technique.

Gene Expression Microarrays

The total RNA was amplified, labeled, and hybridized using a Rat GE 4x44K v3 Microarray Kit (Agilent Technologies, Santa Clara, CA, USA) according to the manufacturer's instructions. All hybridized microarrays were scanned with an Agilent scanner, and the signals of all the probes were calculated using Feature Extraction Software (Agilent Technologies). Employing procedures recommended by Agilent, the raw signal intensities and flags for each probe were calculated from the hybridization intensities and spot information. The present study utilized probes that registered P flags in at least one sample and then calculated intensity based on Z-scores[33] and ratios (non–log-scaled fold change) from the normalized signal intensities of each probe in order to compare the control and experimental samples to identify up- and downregulated genes. Upregulated genes were defined based on Z-scores $\geq$ 2.0 and ratios $\geq$ 1.5-fold, while downregulated genes were defined based on Z-scores ≤ -2.0 and ratios ≤ 0.66. The results were generated from comparisons of control versus glutamate stimulated and of glutamate stimulated versus glutamate stimulated plus tranylcypromine. To determine the significant enrichment of pathways, tools and data provided by the Database for Annotation, Visualization, and Integrated Discovery (DAVID; http://david.abcc.ncifcrf.gov/home.jsp; in the public domain)[34] were used, and a Kyoto Encyclopedia of Genes and Genomes (KEGG)[35] pathway annotation analysis was carried out.

NMDA-Induced Retinal Damage In Vivo

Intravitreal injections of NMDA (Sigma-Aldrich Corp.) were performed in the same fashion as previously described.[36] Briefly, the rats were anesthetized with an intraperitoneal injection of a 1:1 mixture of xylazine hydrochloride (4 mg/kg; Bayer HealthCare, Leverkusen, Germany) and ketamine hydrochloride (10 mg/kg; Daiichi Sankyo Propharma Co., Ltd., Tokyo, Japan). Then, the pupil was dilated with phenylephrine hydrochloride and tropicamide eye drops (Santen Pharmaceutical Co., Ltd., Osaka, Japan), and 20 nmol NMDA with or without tranylcypromine was injected into the vitreous cavity. To assess the inhibitory effect of mitogen-activated protein kinase (MAPK), 100 nmol BIRB796 was intravitreally injected at the same time of NMDA injection. The injections were performed under a microscope using a 33-gauge needle connected to a microsyringe (Ito Corporation, Shizuoka, Japan); the needle was inserted approximately 1.0 mm behind the corneal limbus. Next, either PBS (vehicle control) or 500 mM tranylcypromine (1000 nmol) mixed with 10 mM NMDA (20 nmol) in a total volume of 2.0 μL was injected into the vitreous cavity.

In Vivo Morphometric Analyses

A morphometric analysis to assess the protective effects of tranylcypromine was conducted as previously described.[36] Briefly, 7 days after the NMDA injection, the rats were euthanized by suffocation with carbon dioxide (CO_2); the eyes were enucleated and fixed in 4% paraformaldehyde overnight at 4°C, and then dehydrated and embedded in paraffin ($n = 5$–6 in each condition). Transverse sections (4 μm thick) were prepared from the optic discs, stained with hematoxylin and eosin, and then subjected to the morphometric analysis. The thickness of the inner plexiform layer (IPL) at 1.0 to 1.5 mm from the optic disc was measured, and data from a minimum of three sections for each eye were averaged using a microscope (BX51; Olympus).

Immunohistochemistry

Seven days after the NMDA injection, frozen 14-μm-thick sections were fixed with 4% paraformaldehyde. Following rinses in PBS, samples were permeabilized with 0.02% Triton X-100 in antibody buffer (150 mM NaCl, 50 mM Tris base, 1% BSA, 100 mM L-Lysine, 0.04% Na azide, pH 7.4) and blocked by Image-iT FX Signal Enhancer (Thermo Fisher Scientific) to reduce nonspecific binding. Samples were incubated overnight at 4°C in antibody buffer containing anti-p38 MAPKγ primary antibody (R&D Systems, Minneapolis, MN, USA), washed with PBS, incubated in antibody buffer containing secondary antibody using Alexa Fluor 488 anti-rabbit IgG (no. A-11008, Thermo Fisher Scientific) and 4′,6-diamidino-2-phenylindole (DAPI) for 1 hour at room temperature, and washed with PBS. Samples were mounted using Vectashield mounting medium (no. H-1200; Vector Laboratories, Burlingame, CA, USA), and examined using fluorescence microscopy (BZ-X710; Keyence, Tokyo, Japan).

In Vivo Expression Levels of Caspase 3

The levels of cleaved caspase 3 were evaluated with an immunoblot analysis. Briefly, the retinas ($n = 4$ in each group) were removed 7 days after the NMDA injection and then immediately homogenized using a lysis buffer containing 50 mM Tris-buffered saline (TBS; pH 7.0–7.6), 0.1% sodium deoxycholate, 1 mM ethylenediaminetetraacetic acid (EDTA), and 1% Triton X-100 with complete protease inhibitor cocktail (no. 11836153001; Roche, Basel, Switzerland). Standard immunoblotting was performed as described above.

Retrograde Labeling to Detect the Survival of RGCs

Three days after the NMDA injections, retrograde labeling of RGCs with FluoroGold (FG), in a manner similar to that described previously,[37,38] was performed to assess whether

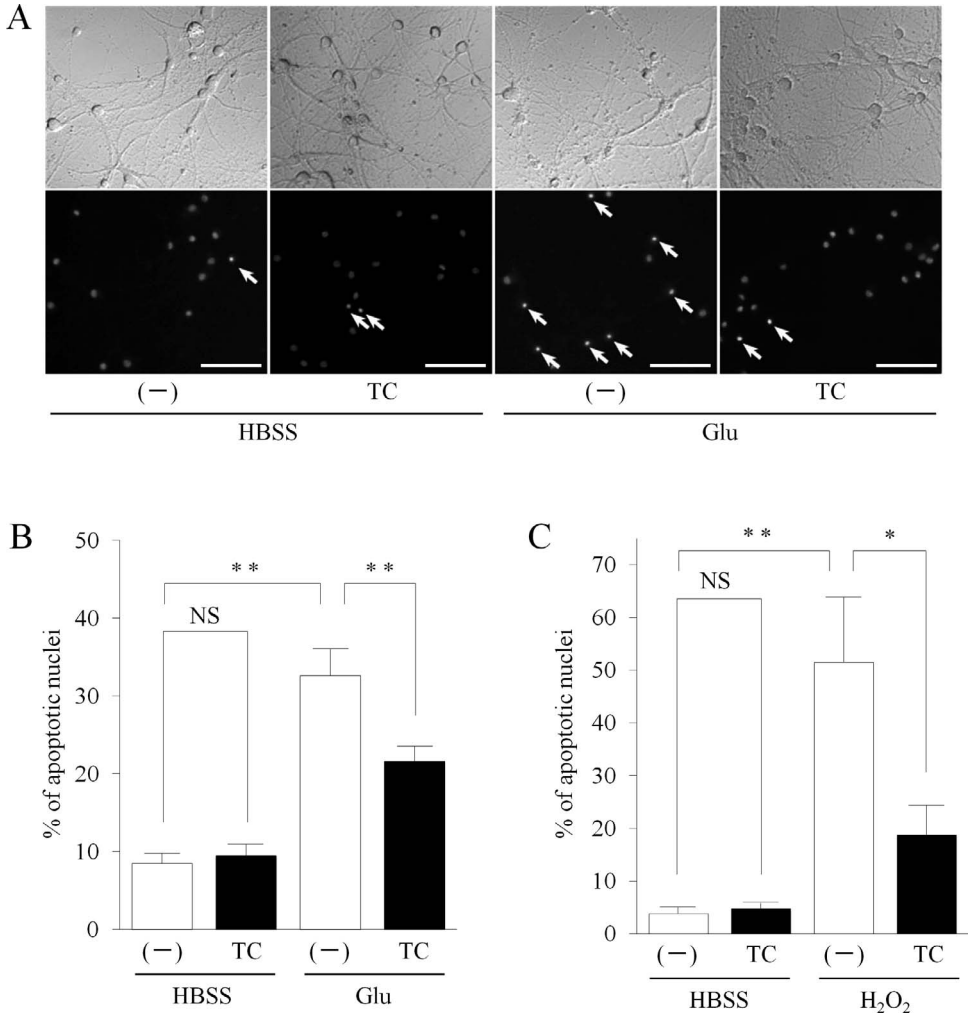

Figure 1. Tranylcypromine (TC) attenuates glutamate (Glu) neurotoxicity- and oxidative stress–induced apoptosis. Fragmented or shrunken nuclei detected by Hoechst staining 24 hours after Glu or oxidative stress under conditions with or without TC. (**A**, **B**) Photo images (*top*) and fluorescence images (*bottom*) of retinal ganglion cells (RGCs) after Glu stimulation. TC significantly suppressed Glu-induced apoptotic cells (indicated by *arrows*) compared with Glu stimulation without TC. (**C**) TC also significantly promoted RGC survival following oxidative stress. All data are represented as means ± standard error (SE). Tukey-Kramer test ($n = 6$–9). $^{*}P < 0.05$, $^{**}P < 0.01$. NS, not significant. *Scale bars*: 50 μm.

tranylcypromine influenced the survival of RGCs. Briefly, after each animal was deeply anesthetized with an intraperitoneal injection of a 1:1 mixture of xylazine hydrochloride (4 mg/kg; Bayer HealthCare) and ketamine hydrochloride (10 mg/kg; Daiichi Sankyo Propharma Co., Ltd.), its head fur was shaved and the skin was incised along the midline to expose the skull and sagittal, coronal, and transverse sutures. Along the bilateral 2-mm diameter, a craniotomy was performed 0.5 mm posterolateral to the sagittal and transverse sutures, and the cerebral content over the superior colliculus was carefully removed with a vacuum pump. Next, a small piece of sterile sponge that was presoaked in 6 μL 6% FG solution was left on the surface of the superior colliculus and the skin wound was sutured and closed.

After the surgery, the rats were kept warm and allowed to recover on their own. Then, 7 days after the NMDA injection, the animals were euthanized, intracardially perfused with PBS to achieve exsanguination, and then perfused with 4% paraformaldehyde. After the perfusion fixation, the eyes were enucleated and fixed with 4% paraformaldehyde overnight at 4°C. Subsequently, the retinas were removed from the sclera and divided into four quadrants (superior, inferior, nasal, and temporal) and mounted on slides. Each quadrant was subdivided into three areas (central, middle, and peripheral) that were 1.0, 2.0, and 3.0 mm from the optic nerve head, respectively. Retinal ganglion cell number was assessed at the point of 1 week ($n = 7$ in each group), 2 weeks ($n = 5$–7 eyes in each group), and 4 weeks ($n = 3$ in each group) after NMDA intravitreal injection. A total of 12 fields per retina were analyzed by counting the number of FG-labeled RGCs with an all-in-one fluorescence microscope (BZ-X710; Keyence) in a masked fashion.

Optic Nerve Crush to Detect Neuroprotective Dose of Tranylcypromine

Eight-week-old male rats were anesthetized by inhalation of 2% isoflurane. After incision of conjunctiva, the optic nerve was bluntly exposed under a microscope. The optic nerve was clamped 1 to 2 mm distal to the globe for 30 seconds with Micro Crip (RS-542; Roboz Surgical Instrument Co., Inc., Gaithersburg, MD, USA), and target reagent was injected intravitreally (5.0 μL/eye) by a Hamilton microsyringe fitted with a 33-gauge needle ($n = 6$ in each condition). For collecting retinas, rats were deeply anaesthetized and euthanized 3 days after optic nerve injury. Total RNA was purified with RNeasy

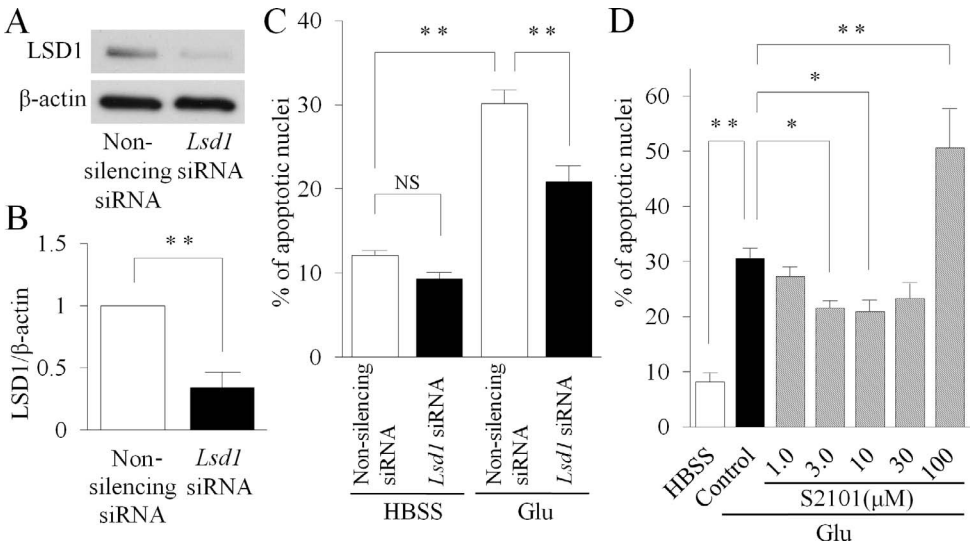

Figure 2. Inhibition of lysine-specific demethylase 1 (LSD1) protects RGCs from apoptosis. (**A**, **B**) Western blot analyses and densitometry showing that *Lsd1*-specific siRNA significantly suppressed the expression of LSD1. Bar graph representing these proportions relative to control ($n = 4$ in each group; Student's *t*-test). (**C**) *Lsd1* siRNA significantly suppressed apoptosis after glutamate (Glu) overload ($n = 4$–6 in each group; Tukey-Kramer test). (**D**) The LSD1-specific pharmacologic inhibitor S2101 also significantly inhibited glutamate (Glu)-induced apoptosis compared with control. All data are represented as means ± SE. Tukey-Kramer test ($n = 4$–6 in each group). $^{*}P < 0.05$, $^{**}P < 0.01$. NS, not significant.

Plus Universal Mini Kit (Qiagen, Valencia, CA, USA), subjected to reverse transcription (PrimeScript RT Master Mix; Takara Bio, Inc., Shiga, Japan), and the resulting cDNA used as the template for a quantitative-PCR reaction (QuantiFast SYBR GreenPCR Kit; Qiagen) performed with Nefl and Gapdh primers. Nefl gene expression was corrected based on Gapdh cDNA.

Statistical Analysis

All data are presented as means ± standard errors. All statistical analyses were performed with either Tukey-Kramer tests or Student's *t*-tests, and the microarray experiments were analyzed with Fisher's exact tests (modified as EASE scores [adjusted Fisher exact probability]). All data analyses were performed using JMP v. 8.0 software (SAS Institute, Inc., Cary, NC, USA), and a confidence level of 95% was considered to indicate statistical significance ($P < 0.05$).

Results

Neuroprotective Effects of Tranylcypromine

Glutamate is a major excitatory neurotransmitter, but it can also act as a neurotoxin during the course of central nervous system (CNS) diseases, such as brain ischemia or injury, multiple sclerosis, Alzheimer's disease, Parkinson's disease, and glaucoma.[39,40] In the present study, glutamate was used to induce the caspase-dependent apoptosis of rat primary cultured RGCs via the NMDA receptor. Hoechst staining revealed that 32.6% of the RGCs that experienced glutamate overload for 2 hours contained shrunken or fragmented nuclei, which are morphologic markers of apoptosis. However, tranylcypromine significantly protected RGCs from glutamate-induced neural cell death (Figs. 1A, 1B).

To determine whether neuronal death induced by other modalities could be prevented by tranylcypromine, the present study exposed RGCs to oxidative stress caused by exposure to H_2O_2 (50 μM) for 30 minutes. B27 supplements without antioxidants rather than the standard B27 supplements used in other experiments were employed in the present study to ensure minimal antioxidant content in the culture medium. There were no significant differences in neuronal survival following the use of either formulation of the B27 supplement (>90%). Upon the exposure of RGCs to H_2O_2 for 30 minutes, 51.4% of the RGCs exhibited apoptotic nuclei; tranylcypromine significantly attenuated neuronal death by 18.6% (Fig. 1C). Thus, tranylcypromine protected RGCs from glutamate neurotoxicity–induced apoptosis as well as apoptosis induced by oxidative stress.

The Inhibition of LSD1 Protects RGCs From Apoptosis

The present study also aimed to determine whether tranylcypromine would have neuroprotective actions via its anti-LSD1 activity. Tranylcypromine possesses dual pharmacologic effects as an LSD1 inhibitor and a monoamine oxidase (MAO) inhibitor, which may be responsible for its antiapoptotic and neuroprotective activities.[41] Thus, the present study investigated neuronal survival after *Lsd1* knockdown.

First, the knockdown effect of the *Lsd1*-specific siRNA was validated with an immunoblotting procedure. Densitometry of the immunoblots revealed that *Lsd1* (*Kdm1a*)-specific siRNA significantly suppressed LSD1 expression by 30.4% compared with the nonsilencing siRNA control (Figs. 2A, 2B). Next, the apoptosis rates of the *Lsd1*-knockdown RGCs were evaluated after glutamate-stimulated neural stress. In RGCs transfected with nonsilencing siRNA, 30.1% of the cells suffered from glutamate-induced apoptosis, but the number of apoptotic RGCs significantly decreased in cells transfected with *Lsd1*-specific siRNA (Fig. 2C). Similarly, the pharmacologic inhibition of LSD1 with S2101, which is structurally related to tranylcypromine but has a higher affinity for LSD1 despite a substantially weaker effect on MAOs,[42] promoted cell survival following glutamate-induced stress (Fig. 2D). At 100 μM, S2101 showed a high rate of apoptotic nuclei in RGCs, and this cytotoxicity of S2101 would be a secondary and adverse effect. Taken together, these findings indicate that the suppression of LSD1 activity may contribute to neuroprotection following apoptotic stress.

Table 1. KEGG Pathway Functional Classification for Downstream Involved in Tranylcypromine

Term	*P* Value
rno04666: Fc-gamma R-mediated phagocytosis	0.010
rno04722: Neurotrophin signaling pathway	0.026
rno00230: Purine metabolism	0.044
rno04914: Progesterone-mediated oocyte maturation	0.074
rno04144: Endocytosis	0.084

KEGG, Kyoto Encyclopedia of Genes and Genomes. EASE score, modified Fisher's exact P value < 0.05.

Target Pathways and Genes Involved in the Tranylcypromine-Induced Survival of RGCs

Next, the present study investigated the signaling pathways involved in the neuroprotective effects of tranylcypromine. To identify the gene expression changes induced by tranylcypromine in RGCs, a microarray analysis evaluating 26,930 gene expression changes was carried out. Because previous studies have shown that LSD1 suppresses gene transcription via a demethylation reaction of histone H3 lysine 4,[26,27] it was hypothesized that the genes whose expression is enhanced by tranylcypromine and simultaneously decreased by glutamate administration could be promising candidates as gene targets for the regulation of neuronal survival. The microarray data were reported as Z-scores and ratios and revealed that 110 genes satisfied these criteria.

Additionally, a KEGG pathway annotation analysis was performed using DAVID. This analysis revealed the significant detection of three enriched KEGG pathway terms for functional classification that were associated with the 110 gene candidates identified in the present study; these terms were involved in Fc-gamma R–mediated phagocytosis, the neurotrophin signaling pathway, and purine metabolism (Table 1). The details of the expression profiles are listed in Table 2. Next, the analyses focused on two neurotrophin signaling molecules, v-akt murine thymoma viral oncogene homolog 1 (Akt1) and mitogen-activated protein kinase 12 (p38 MAPKγ), because the phosphatidylinositol-3-kinase (PI3K)/Akt/mTOR and MAPK pathways are key signaling pathways for cell survival and antiapoptotic activity.[43–46]

Tranylcypromine Enhances RGC Survival via P38 MAPK Activity

The present study also investigated changes in the activity of two candidate pathways involved in RGC survival as well as the expression and phosphorylation statuses of Akt and total p38 MAPKs using immunoblot analyses. The ratios of total Akt/β-actin and phospho-Akt/total Akt were unchanged following the administration of tranylcypromine in both the control and glutamate-induced stress conditions (Figs. 3A–C). Similarly, the total p38 MAPK expression and phosphor/p38 MAPK ratio did not show any statistical changes following the application of either tranylcypromine or glutamate stress (Figs. 3D–F). On the other hand, the expression of p38 MAPKγ, which is one of four p38 MAPK subtypes, was significantly suppressed by glutamate administration; this suppression was ameliorated by tranylcypromine (Figs. 3J, 3K). Additionally, microarray data and immunoblot analysis showed that the expression of p38 MAPKα or p38 MAPKβ was not affected by tranylcypromine (Figs. 3G–I; Supplementary Table S1). These findings suggest that the neuroprotective effects of tranylcypromine might be profoundly and specifically affected by p38 MAPKγ rather than the total p38 MAPKs.

To elucidate whether p38 MAPKγ or Akt protects RGCs from glutamate overload, the cell survival rates after the pharmacologic inhibition of Akt or p38 MAPKγ were assessed using wortmannin as a potent and selective inhibitor of PI3K, and BIRB796 and SB203580 as specific inhibitors of p38 MAPK. Wortmannin had no effect on RGC survival in either the glutamate stress or glutamate with tranylcypromine condition (Fig. 4A). Although there were no significant effects of SB203580, the p38 MAPK inhibitor BIRB796, which inhibits all four p38 MAPK subtypes,[47] clearly blocked the neuroprotective effects of tranylcypromine against glutamate-induced

Table 2. Candidate Genes Associated With Tranylcypromine-Induced Neuroprotection

			Control vs. Glu		Glu vs. Glu + TC	
GenBank Accession	Gene Symbol	Gene Name	Z-Score	Ratio	Z-Score	Ratio
Fc-gamma R-mediated phagocytosis						
NM_031146	arpc1a	actin-related protein 2/3 complex, subunit 1A	−2.47	0.50	2.06	2.06
XM_001067293	LOC688430	cofilin 1, nonmuscle; similar to cofilin-1, cofilin, nonmuscle isoform	−2.11	0.61	3.80	2.89
AF503609	PPAP2A	phosphatidic acid phosphatase type 2A	−2.62	0.11	2.76	9.52
NM_033230	akt1	v-akt murine thymoma viral oncogene homolog 1	−3.01	0.43	2.12	2.11
Neurotrophin signaling pathway						
NM_053409	MAGED1	melanoma antigen, family D, 1	−2.45	0.56	2.12	1.81
NM_021746	MAPK12	mitogen-activated protein kinase 12	−2.10	0.56	2.84	2.71
NM_031767	Sort1	sortilin 1	−2.40	0.51	2.15	2.13
NM_033230	akt1	v-akt murine thymoma viral oncogene homolog 1	−3.01	0.43	2.12	2.11
Purine metabolism						
NM_053396	ADCY7	adenylate cyclase 7	−2.43	0.13	2.55	8.01
NM_022710	pde1b	phosphodiesterase 1B, calmodulin dependent	−2.18	0.43	2.32	2.93
NM_001014259	POLR3K	polymerase (RNA) III, DNA directed, polypeptide K, 12.3 kDa	−2.05	0.61	2.38	1.94
NM_001105791	PFAS	Similar to phosphoribosylformylglycinamidine synthase; phosphoribosylformylglycinamidine synthase	−2.40	0.40	2.13	2.68

Glu, glutamate; TC, tranylcypromine.

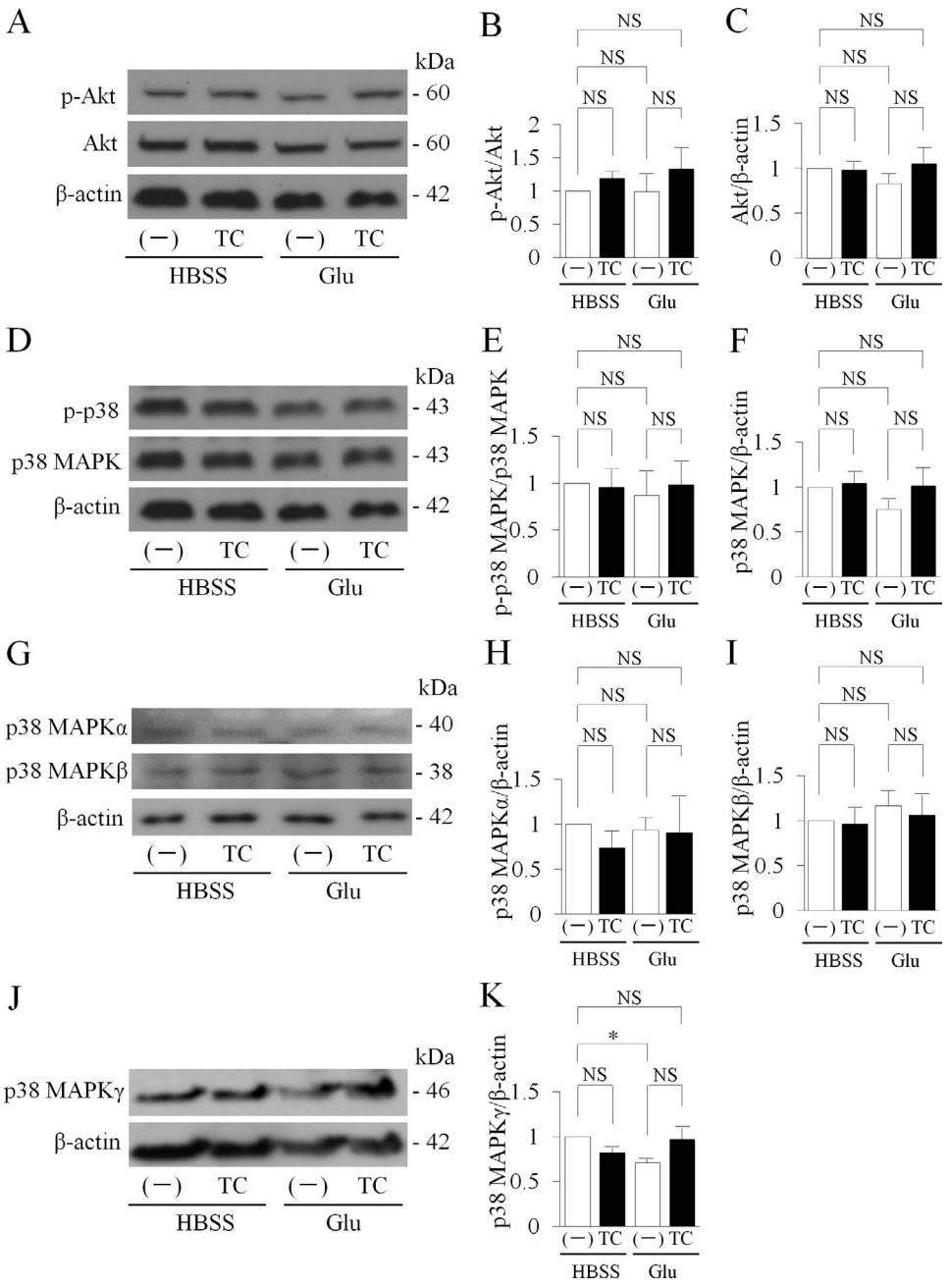

Figure 3. Tranylcypromine (TC) promotes mitogen-activated protein kinase 12 (p38 MAPKγ) expression under conditions of glutamate (Glu)-induced stress. (**A–C**) Western blot analyses and densitometry showing that Glu had no effect on the expression of Akt. TC did not influence Akt expression or the phosphorylation of Akt. (**D–F**) Glu had no effect on the expression of total p38 MAPK or its phosphorylation status. TC did not change total p38 MAPK expression or its phosphorylation status. (**G–I**) The expression of p38 MAPKα or p38 MAPKβ was not affected by TC. (**J**, **K**) However, TC significantly promoted the expression of p38 MAPKγ. All data are represented as means ± SE. Tukey-Kramer test ($n = 5$–7 for each experiment, except p38 MAPKα/β experiments [$n = 3$]). *$P < 0.05$. NS, not significant.

RGC death (Fig. 4B). SB203580 is a typical inhibitor of p38 MAPKα and p38 MAPKβ but not p38 MAPKγ or p38 MAPKδ.[48,49] Thus, the present pharmacologic results supported the proposed hypothesis that tranylcypromine contributes to RGC survival via alterations of p38 MAPKγ activity.

Tranylcypromine Promotes the In Vivo Survival of RGCs

Finally, the present study investigated whether tranylcypromine regulates in vivo RGC survival under conditions of stress. First, morphologic changes in the retinas after tranylcypromine administration were assessed using an in vivo rat model of NMDA-induced retinal damage. Intravitreal injections of NMDA significantly reduced IPL thickness compared with intravitreal injections of PBS. However, the NMDA-injected retinas that received treatment with tranylcypromine maintained IPL thickness to a degree similar to that of the control retinas (Fig. 5). Second, because the expression levels of the caspase family generally reflect apoptotic activity,[50,51] the present study aimed to determine the level of NMDA-induced caspase 3 cleavage, which is an indicator of caspase 3 activation,

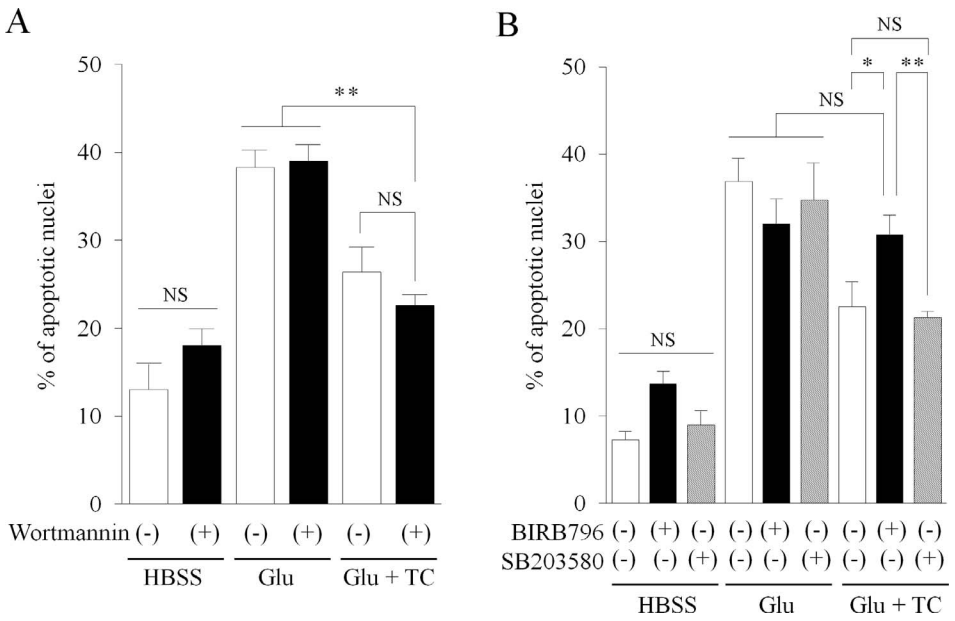

Figure 4. Tranylcypromine (TC) contributes to RGC survival via p38MAPKγ activity. RGC apoptosis was evaluated based on morphologic changes of the nuclei. (**A**) Wortmannin had no effect on the survival ratio in either the glutamate (Glu)-stressed or Glu with TC (Glu + TC) conditions. (**B**) Similarly, SB203580, which is a p38α/p38β-specific inhibitor, did not have an effect in the Glu + TC condition, but the protective effects of TC on RGCs were attenuated by the p38MAPK inhibitor BIRB796. This suggests that TC may protect neurons via alterations in p38MAPK isoforms, except for p38α and p38β. All data are represented as means ± SE. Student's *t*-test ($n = 4$ in each group). $^{*}P < 0.05$, $^{**}P < 0.01$. NS, not significant.

following the administration of tranylcypromine using immunoblot analyses. In the retinas treated with NMDA and vehicle, there was a significant increase in the levels of cleaved caspase 3 at 18 hours after the NMDA injection; this activity was significantly suppressed in the tranylcypromine-treated retinas (Fig. 6). Taken together, these findings indicate that the intravitreal tranylcypromine injections exerted neuroprotective effects within intracellular apoptotic signaling pathways and suppressed morphologic changes in the retina.

Additionally, we investigated whether tranylcypromine showed modification effects of p38 MAPKγ expression in vivo similar to those in vitro. Seven days after NMDA-induced retinal neurotoxicity, p38 MAPKγ expression was significantly suppressed in the RGC layers. However, this suppression was recovered by tranylcypromine and its effect was canceled by BIRB796 (Fig. 6C), suggesting that tranylcypromine might similarly show an in vivo antiapoptotic effect via p38 MAPKγ activity.

Next, the effective concentration of tranylcypromine for retinal neuroprotection was assessed. Three days after optic nerve crush, the light neurofilament (NF-L) gene expression after tranylcypromine treatment increased dose-dependently, and 1000-nmol injection of tranylcypromine showed an increase in NF-L expression similar to BDNF (5.0 μg/eye) positive control (Supplementary Fig. S1).

Finally, the present study assessed the degree to which tranylcypromine protects RGCs from NMDA-induced retinal neurotoxicity. The actual numbers of RGCs that were labeled in a retrograde manner by FG were counted in the retinas of sham-treated, tranylcypromine-treated, NMDA-treated, and

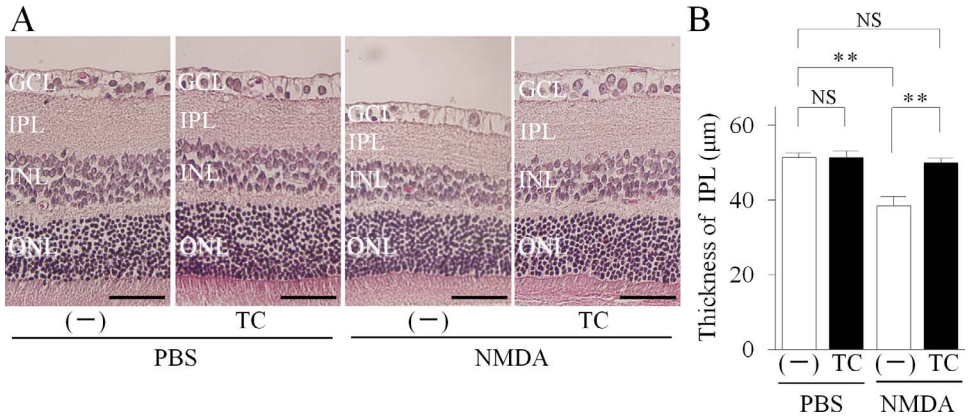

Figure 5. Morphologic protection of retinal cells from N-methyl-D-aspartate (NMDA)-induced stress by intravitreal injections of tranylcypromine (TC). (**A**) Light microscopic images of retinal section samples showing a thick inner plexiform layer (IPL) after TC treatment, even in the NMDA-stressed condition. (**B**) IPL thickness following NMDA administration was significantly thinner than that after the administration of phosphate-buffered saline (PBS). However, TC injections fully recovered the NMDA-induced retinal damage. All data are represented as means ± SE. Tukey-Kramer test ($n = 5$–6 for each). $^{**}P < 0.01$. NS, not significant. *Scale bars*: 50 μm. GCL, ganglion cell layer; INL, inner nuclear layer; ONL, outer nuclear layer.

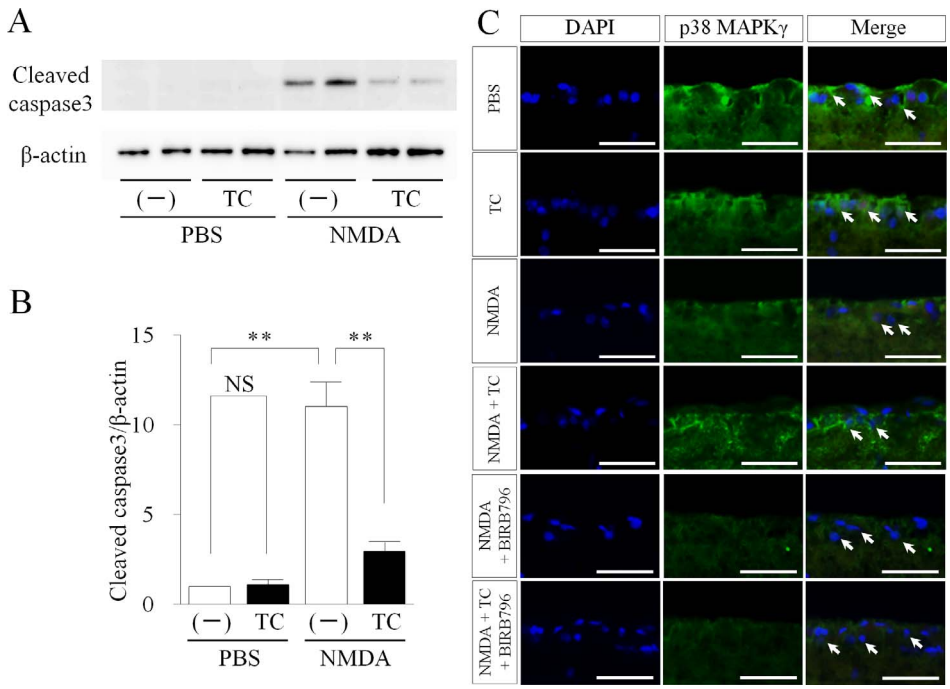

Figure 6. Tranylcypromine (TC) suppresses caspase 3 activity and recovers p38 MAPKγ expression in the retina after NMDA-induced injury. (**A**, **B**) Western blot analyses and densitometry showing the significant inhibition of the apoptotic signal cleaved caspase 3 by TC. (**C**) Whereas p38 MAPKγ expression was significantly suppressed by NMDA in the retinal ganglion cell layer (indicated by *arrows*), this suppression was ameliorated by TC. Also, BIRB796 inhibited TC-induced p38γ recovery. All data are represented as means ± SE. Tukey-Kramer test ($n = 4$ for each). $^{**}P < 0.01$. NS, not significant. *Scale bars*: 50 μm.

NMDA- and tranylcypromine-treated animals. At 7 days after the intravitreal injections of NMDA, the numbers of RGCs in the NMDA-treated group decreased by 21.5% and 29.9% in the middle and peripheral regions of the retina, respectively. In contrast, the numbers of RGCs in the NMDA- and tranylcypromine-treated groups significantly increased by 49.9% and 53.3% in the middle and peripheral regions, respectively (Figs. 7A–C). Also, single injection of tranylcypromine enhanced RGC survival for at least 2 weeks in the middle and peripheral regions of the retina (Figs. 7D, 7E). Thus, intravitreal tranylcypromine treatment enhanced RGC survival after retinal injury via the attenuation of NMDA neurotoxicity.

Discussion

The findings of the present study demonstrated that a novel neuroprotective drug, tranylcypromine, exerted suppressive activity against LSD1. Lysine-specific demethylase 1 is a well-known member of the flavin-containing amine oxidase family that represses transcription by removing the methyl group from monomethylated and dimethylated lysine 4 of histone H3.[26,27] To our knowledge, this is the first study to report that tranylcypromine suppressed neuronal cell death induced by glutamate or oxidative stress via the inhibition of LSD1. Furthermore, the present study demonstrated that the intravitreal administration of tranylcypromine significantly protected RGCs in an in vivo rat model of NMDA-induced excitotoxicity that led to a significant loss of RGCs. Thus, the transcriptional and epigenetic regulation induced by tranylcypromine might be a potential therapeutic target for the treatment of neurodegenerative diseases.

The data presented here indicate that the neuroprotective effects of tranylcypromine are related to the modulation of LSD1 activity. Previous studies have shown that LSD1 influences cell proliferation, is prosurvival,[52,53] aids in neurite morphogenesis,[54] and promotes neural differentiation and development.[55] It has also been shown that the inhibition of LSD1 by tranylcypromine modulates neural stem cell proliferation in the mouse brain[53] and changes zebrafish lateral line neuromast development.[56] Interestingly, the present findings indicate that tranylcypromine also significantly benefited cell survival in the mammalian CNS.

Tranylcypromine is a potent dual-action drug that inhibits the activities of LSD1 and MAOs.[57,58] Monoamine oxidases catalyze the oxidative deamination of dietary amines and monoamine neurotransmitters and, in turn, produce the by-products of MAO-related reactions, including 3,4-dihydroxyphenylglycolaldehyde (DOPEGAL) and H_2O_2. These potentially neurotoxic metabolites lead to the apoptosis of neuronal cells and are considered to be possible causes of neurodegenerative diseases such as Parkinson's disease and Alzheimer's disease.[59,60] Therefore, inactivation of MAO is thought to be a good strategy for the protection of neuronal cells in vitro and in vivo.[61,62] In fact, MAO inhibitors such as l-deprenyl (selegiline) and (R)-N-(prop-2-ynyl)-2,3-dihydro-1H-inden-1-amine (rasagiline) have become archived pharmacologic therapeutic options for human neuropsychiatric diseases such as Parkinson's disease,[63–65] treatment-resistant depression,[66] and anxiety disorders.[67]

To clarify whether LSD1 and/or MAO were important factors in the neuroprotective effects provided by tranylcypromine, neuronal survival was investigated in *Lsd1*-knockdown samples using *Lsd1*-specific siRNA or via pharmacologic inhibition with S2101, which has a potent affinity for LSD1 despite a substantially weaker affinity for MAOs than tranylcypromine.[42] Both experimental conditions revealed that the suppression of LSD1 significantly diminished the protective effects of tranylcypromine on RGCs, which implies that LSD1 is more important for neuroprotection than MAO. To the best of

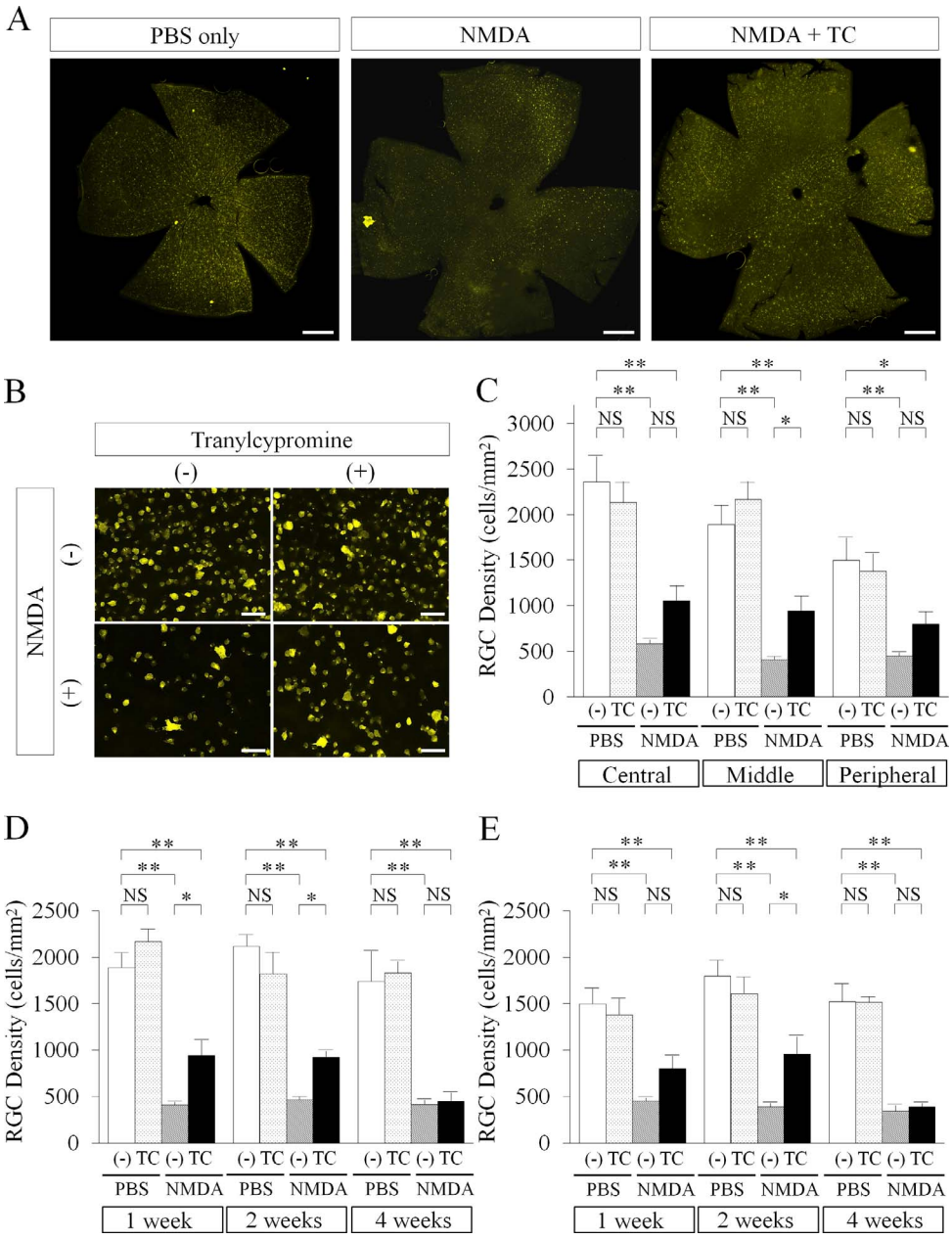

Figure 7. Tranylcypromine (TC) has significant neuroprotective effects against NMDA-induced apoptosis in vivo. FluoroGold-retrograde labeling of RGCs. (**A**, **B**) Flat-mount samples showing significant RGC loss after intravitreal NMDA injections. However, the RGCs were rescued by TC treatment. (**C**) Actual RGC numbers showing statistically greater numbers following TC treatment in the midregion of the retina (**D**, **E**) Single injection of TC enhanced RGC survival for at least 2 weeks in the middle region (**D**) and in the peripheral region (**E**). All data are represented as means ± SE. Tukey-Kramer test. $^{*}P < 0.05$, $^{**}P < 0.01$. NS, not significant. *Scale bars*: 1.0 mm (**A**); 50 μm (**B**).

our knowledge, this is the first study to demonstrate that the inhibition of LSD1 promotes neuroprotection.

However, the manner in which LSD1 regulates neuronal survival remains unclear. Because LSD1 is an important molecule involved in the epigenetic regulation of gene transcription,[26,27] the modulation of downstream gene expression was assessed in the present study. Exhaustive microarray analyses revealed that p38 MAPKγ is one of the key players involved in the neuroprotection afforded by LSD1. Mitogen-activated protein kinases such as extracellular signal–regulated protein kinases 1 and 2 (ERK1/2), c-jun N-terminal kinase (JNK), and p38 are well-known factors associated with the survival, proliferation, and differentiation of neuronal[68,69] and nonneuronal[70,71] cells. Recently, Jiang et al.[72] reported that the inhibition of p38 MAPK had a neuroprotective effect via crosstalk with nuclear factor kappa-light-chain enhancer of activated B cells (NF-κB) p65 in a rat model of retinal ischemia/reperfusion injury. Interestingly, the p38 MAPK family consists of four major isoforms, p38α, p38β, p38γ, and p38δ, which are encoded by independent genes and are considered to have isoform-specific functions as well as functional redundancies.[73]

Using cells within the CNS, several studies have demonstrated that the p38 MAPKα isoform is a relatively more important contributor to stressor-induced proinflammatory cytokine production and neurotoxicity compared with the p38β isoform.[74–76] Several studies have reported that SB203580, a typical inhibitor of p38 MAPKα and p38 MAPKβ, rescues RGCs from NMDA and optic nerve injury, suggesting

the involvement of p38 MAPKα and p38 MAPKβ in RGC survival. [77,78] However, the roles of the other p38 isoforms in neuronal cells have yet to be elucidated. Whereas other studies have found that the p38α isoform leads to neuronal death,[76] the present data demonstrated that an increased level of phosphorylated p38γ (and/or p38δ) enhanced the survival of primary RGCs. Interestingly, Ferrari et al.[79] recently identified a similar phenomenon showing that the survival effects of p38γ are opposite to those of p38α in vascular endothelial cells. P38α mediates apoptotic signaling from inducers of endothelial cell apoptosis, such as transforming growth factor-β (TGF-β), but p38γ induces survival signaling.[79] Further studies are needed to define the relative importance of neuronal p38γ and p38δ in excitotoxicity-stimulated RGCs.

Finally, the present study investigated whether tranylcypromine would regulate RGC survival in vivo. Intravitreal injections of tranylcypromine not only sustained the thickness of the IPL but also reduced RGC loss after overloading NMDA receptors in the rat retina. Thus, the in vivo targeting of LSD1 activity by tranylcypromine may protect RGCs following retinal damage. Clinical usefulness of systemic tranylcypromine in the treatment of mood and anxiety disorders was seriously limited because of adverse effects such as orthostatic hypotension, sleep disturbances, and nervousness/agitation, and the potential risk of hypertensive crisis and liver toxicity caused by interactions with tyramine-rich foods and sympathomimetic and serotoninergic substances.[80,81] However, ocular topical administration including intravitreal injection may minimize the risk of systemic adverse events. Taken together, these in vitro and in vivo data strongly support that epigenetic regulation of transcriptional modulators affecting the signaling pathways critical for regulating neuronal survival may be a hopeful therapeutic target for neurodegenerative eye diseases.

In conclusion, the present study found that tranylcypromine, which is a typical LSD1 inhibitor, exerted significant neuroprotective effects on RGCs by promoting neuronal expression of the p38 MAPKγ isoform, which might be one of main players in the enhancement of neuronal survival. Additionally, the intravitreal administration of tranylcypromine led to the neuroprotection of RGCs in a rat model of NMDA-induced excitotoxicity stress, which suggests that suppression of LSD1 may be a good therapeutic target for the treatment of neurodegenerative diseases, such as glaucoma.

Acknowledgments

The authors thank Rei Shiromoto and Miyuki Inoue for technical assistance.

Supported by JSPS KAKENHI Grant 26293375 (to HT), 15K06781 (to HH), 16K11290 (to KI), 23116009 (to MN), and 25430178 (to SH); Takeda Science Foundation (to HH and to MN), and Encourage Project Fund from Kumamoto University Research Project Stem Cell-Based Tissue Regeneration Research and Education Unit (to KI).

Disclosure: **T. Tsutsumi**, None; **K. Iwao**, None; **H. Hayashi**, None; **T. Kirihara**, None; **T. Kawaji**, None; **T. Inoue**, None; **S. Hino**, None; **M. Nakao**, None; **H. Tanihara**, None

References

1. Quigley HA, Nickells RW, Kerrigan LA, Pease ME, Thibault DJ, Zack DJ. Retinal ganglion cell death in experimental glaucoma and after axotomy occurs by apoptosis. *Invest Ophthalmol Vis Sci*. 1995;36:774–786.
2. Quigley HA. Number of people with glaucoma worldwide. *Br J Ophthalmol*. 1996;80:389–393.
3. Resnikoff S, Pascolini D, Etya'ale D, et al. Global data on visual impairment in the year 2002. *Bull World Health Organ*. 2004; 82:844–851.
4. Quigley HA, Broman AT. The number of people with glaucoma worldwide in 2010 and 2020. *Br J Ophthalmol*. 2006;90:262–267.
5. Heijl A, Leske MC, Bengtsson B, Hyman L, Bengtsson B, Hussein M; Early Manifest Glaucoma Trial Group. Reduction of intraocular pressure and glaucoma progression: results from the Early Manifest Glaucoma Trial. *Arch Ophthalmol*. 2002; 120:1268–1279.
6. Nouri-Mahdavi K, Hoffman D, Coleman AL, et al.; Advanced Glaucoma Intervention Study. Predictive factors for glaucomatous visual field progression in the Advanced Glaucoma Intervention Study. *Ophthalmology*. 2004;111:1627–1635.
7. De Moraes CG, Demirel S, Gardiner SK, et al. Effect of treatment on the rate of visual field change in the ocular hypertension treatment study observation group. *Invest Ophthalmol Vis Sci*. 2012;53:1704–1709.
8. Leydhecker W, Akiyama K, Neumann HG. Der intraokulare Druck gesunder menschlicher Augen. *Klin Monbl Augenheilkd Augenarztl Fortbild*. 1958;133:662–670.
9. He M, Foster PJ, Ge J, et al. Prevalence and clinical characteristics of glaucoma in adult Chinese: a population-based study in Liwan District Guangzhou. *Invest Ophthalmol Vis Sci*. 2006;47:2782–2788.
10. Kim CS, Seong GJ, Lee NH, Song KC; Namil Study Group Korean Glaucoma Society. Prevalence of primary open-angle glaucoma in central South Korea the Namil study. *Ophthalmology*. 2011;118:1024–1030.
11. Narayanaswamy A, Baskaran M, Zheng Y, et al. The prevalence and types of glaucoma in an urban Indian population: the Singapore Indian Eye Study. *Invest Ophthalmol Vis Sci*. 2013; 54:4621–4627.
12. Iwase A, Suzuki Y, Araie M; Tajimi Study Group. Characteristics of undiagnosed primary open-angle glaucoma: the Tajimi Study. *Ophthalmic Epidemiol*. 2014;21:39–44.
13. Hamard P, Hamard H, Dufaux J, Quesnot S. Optic nerve head blood flow using a laser Doppler velocimeter and haemorheology in primary open angle glaucoma and normal pressure glaucoma. *Br J Ophthalmol*. 1994;78:449–453.
14. Tielsch JM, Katz J, Sommer A, Quigley HA, Javitt JC. Family history and risk of primary open angle glaucoma. The Baltimore Eye Survey. *Arch Ophthalmol*. 1994;112:69–73.
15. Wang X, Harmon J, Zabrieskie N, et al. Using the Utah Population Database to assess familial risk of primary open angle glaucoma. *Vision Res*. 2010;50:2391–2395.
16. Ren R, Jonas JB, Tian G, et al. Cerebrospinal fluid pressure in glaucoma: a prospective study. *Ophthalmology*. 2010;117: 259–266.
17. Collaborative Normal-Tension Glaucoma Study Group. The effectiveness of intraocular pressure reduction in the treatment of normal-tension glaucoma. *Am J Ophthalmol*. 1998; 126:498–505.
18. Riggs AD, Porter TN. Overview of epigenetic mechanisms. Epigenetic Mechanisms of Gene Regulation. In: Russo VEA, Martienssen RA, Riggs AD, eds. *Epigenetic Mechanisms of Gene Regulation*. New York: Cold Spring Harbor Monograph Archive; 1996;32:29–45.
19. van Holde KE. *Chromatin*. New York: Springer; 1988:111–148.
20. Wysocka J, Milne TA, Allis CD, Taking LSD. 1 to a new high. *Cell*. 2005;122:654–658.
21. Pelzel HR, Schlamp CL, Nickells RW. Histone H4 deacetylation plays a critical role in early gene silencing during neuronal apoptosis. *BMC Neurosci*. 2010;11:62.

22. Biermann J, Grieshaber P, Goebel U, et al. Valproic acid-mediated neuroprotection and regeneration in injured retinal ganglion cells. *Invest Ophthalmol Vis Sci*. 2010;51:526–534.
23. Kimura A, Guo X, Noro T, et al. Valproic acid prevents retinal degeneration in a murine model of normal tension glaucoma. *Neurosci Lett*. 2015;588:108–113.
24. Kimura A, Namekata K, Guo X, et al. Valproic acid prevents NMDA-induced retinal ganglion cell death via stimulation of neuronal TrkB receptor signaling. *Am J Pathol*. 2015;185:756–764.
25. Schmitt HM, Pelzel HR, Schlamp CL, Nickells RW. Histone deacetylase 3 (HDAC3) plays an important role in retinal ganglion cell death after acute optic nerve injury. *Mol Neurodegener*. 2014;9:39.
26. Shi Y, Lan F, Matson C, et al. Histone demethylation mediated by the nuclear amine oxidase homolog LSD1. *Cell*. 2004;119:941–953.
27. Forneris F, Binda C, Vanoni MA, Battaglioli E, Mattevi A. Human histone demethylase LSD1 reads the histone code. *J Biol Chem*. 2005;280:41360–41365.
28. Barres BA, Silverstein BE, Corey DP, Chun LL. Immunological, morphological and electrophysiological variation among retinal ganglion cells purified by panning. *Neuron*. 1988;1:791–803.
29. Goldberg JL, Espinosa JS, Xu Y, Davidson N, Kovacs GT, Barres BA. Retinal ganglion cells do not extend axons by default: promotion by neurotrophic signaling and electrical activity. *Neuron*. 2002;33:689–702.
30. Hayashi H, Campenot RB, Vance DE, Vance JE. Apolipoprotein E-containing lipoproteins protect neurons from apoptosis via a signaling pathway involving low-density lipoprotein receptor-related protein-1. *J Neurosci*. 2007;27:1933–1941.
31. Hayashi H, Eguchi Y, Fukuchi-Nakaishi Y, et al. A potential neuroprotective role of apolipoprotein E-containing lipoproteins through low density lipoprotein receptor-related protein 1 in normal tension glaucoma. *J Biol Chem*. 2012;287:25395–25406.
32. Henson MA, Roberts AC, Perez-Otano I, Philpot BD. Influence of the NR3A subunit on NMDA receptor functions. *Prog Neurobiol*. 2010;91:23–37.
33. Quackenbush J. Microarray data normalization and transformation. *Nat Genet*. 2002;32(suppl):496–501.
34. Huang da W, Sherman BT, Lempicki RA. Bioinformatics enrichment tools: paths toward the comprehensive functional analysis of large gene lists. *Nucleic Acids Res*. 2009;37:1–13.
35. Kanehisa M, Goto S. KEGG: Kyoto Encyclopedia of Genes and Genomes. *Nucleic Acids Res*. 2000;28:27–30.
36. Morizane C, Adachi K, Furutani I, et al. N(omega)-nitro-L-arginine methyl ester protects retinal neurons against N-methyl-D-aspartate-induced neurotoxicity in vivo. *Eur J Pharmacol*. 1997;328:45–49.
37. Chiu K, Lau WM, Yeung SC, Chang RC, So KF. Retrograde labeling of retinal ganglion cells by application of fluorogold on the surface of superior colliculus. *J Vis Exp*. 2008;16:819.
38. Wang Y, Brown DP Jr, Duan Y, Kong W, Watson BD, Goldberg JL. A novel rodent model of posterior ischemic optic neuropathy. *JAMA Ophthalmol*. 2013;131:194–204.
39. Harada T, Harada C, Nakamura K, et al. The potential role of glutamate transporters in the pathogenesis of normal tension glaucoma. *J Clin Invest*. 2007;117:1763–1770.
40. Lau A, Tymianski M. Glutamate receptors neurotoxicity and neurodegeneration. *Pflugers Arch*. 2010;460:525–542.
41. Magyar K. (-)-Deprenyl, a selective MAO-B inhibitor, with apoptotic and anti-apoptotic properties. *Neurotoxicology*. 2004;25:233–242.
42. Hino S, Sakamoto A, Nagaoka K, et al. FAD-dependent lysine-specific demethylase-1 regulates cellular energy expenditure. *Nat Commun*. 2012;3:758.
43. Martindale JL, Holbrook NJ. Cellular response to oxidative stress: signaling for suicide and survival. *J Cell Physiol*. 2002;192:1–15.
44. Irani K. Oxidant signaling in vascular cell growth, death and survival: a review of the roles of reactive oxygen species in smooth muscle and endothelial cell mitogenic and apoptotic signaling. *Circ Res*. 2000;87:179–183.
45. Das DK, Maulik N. Conversion of death signal into survival signal by redox signaling. *Biochemistry*. 2004;69:10–17.
46. Chan S. Targeting the mammalian target of rapamycin (mTOR): a new approach to treating cancer. *Br J Cancer*. 2004;91:1420–1424.
47. Kuma Y, Sabio G, Bain J, Shpiro N, Marquez R, Cuenda A. BIRB796 inhibits all p38 MAPK isoforms in vitro and in vivo. *J Biol Chem*. 2005;280:19472–19479.
48. Goedert M, Cuenda A, Craxton M, Jakes R, Cohen P. Activation of the novel stress-activated protein kinase SAPK4 by cytokines and cellular stresses is mediated by SKK3 (MKK6); comparison of its substrate specificity with that of other SAP kinases. *EMBO J*. 1997;16:3563–3571.
49. Cohen P, Goedert M. Engineering protein kinases with distinct nucleotide specificities and inhibitor sensitivities by mutation of a single amino acid. *Chem Biol*. 1998;5:161–164.
50. Namura S, Zhu J, Fink K, et al. Activation and cleavage of caspase-3 in apoptosis induced by experimental cerebral ischemia. *J Neurosci*. 1998;18:3659–3668.
51. Porter AG, Janicke RU. Emerging roles of caspase-3 in apoptosis. *Cell Death Differ*. 1999;6:99–104.
52. Scoumanne A, Chen X. The lysine-specific demethylase 1 is required for cell proliferation in both p53-dependent and -independent manners. *J Biol Chem*. 2007;282:15471–15475.
53. Sun G, Alzayady K, Stewart R, et al. Histone demethylase LSD1 regulates neural stem cell proliferation. *Mol Cell Biol*. 2010;30:1997–2005.
54. Zibetti C, Adamo A, Binda C, et al. Alternative splicing of the histone demethylase LSD1/KDM1 contributes to the modulation of neurite morphogenesis in the mammalian nervous system. *J Neurosci*. 2010;30:2521–2532.
55. Fuentes P, Canovas J, Berndt FA, Noctor SC, Kukuljan M. CoREST/LSD1 control the development of pyramidal cortical neurons. *Cereb Cortex*. 2012;22:1431–1441.
56. He Y, Yu H, Sun S, et al. Trans-2-phenylcyclopropylamine regulates zebrafish lateral line neuromast development mediated by depression of LSD1 activity. *Int J Dev Biol*. 2013;57:365–373.
57. Lee MG, Wynder C, Schmidt DM, McCafferty DG, Shiekhattar R. Histone H3 lysine 4 demethylation is a target of nonselective antidepressive medications. *Chem Biol*. 2006;13:563–567.
58. Schmidt DM. McCafferty DG. trans-2-Phenylcyclopropylamine is a mechanism-based inactivator of the histone demethylase LSD1. *Biochemistry*. 2007;46:4408–4416.
59. Butterfield DA. β-Amyloid-associated free radical oxidative stress and neurotoxicity: implications for Alzheimer's disease. *Chem Res Toxicol*. 1997;10:495–506.
60. Burke WJ, Li SW, Chung HD, et al. Neurotoxicity of MAO metabolites of catecholamine neurotransmitters: role in neurodegenerative diseases. *Neurotoxicology*. 2004;25:101–115.
61. Huang W, Chen Y, Shohami E, Weinstock M. Neuroprotective effect of rasagiline, a selective monoamine oxidase-B inhibitor, against closed head injury in the mouse. *Eur J Pharmacol*. 1999;366:127–135.

Investigative Ophthalmology & Visual Science

62. Speiser Z, Mayk A, Eliash S, Cohen S. Studies with rasagiline, a MAO-B inhibitor, in experimental focal ischemia in the rat. *J Neural Transm*. 1999;106:593–606.
63. Parkinson Study Group. A controlled trial of rasagiline in early Parkinson disease: the TEMPO Study. *Arch Neurol*. 2002;59:1937–1943.
64. Shoulson I, Oakes D, Fahn S, et al.; Parkinson Study Group. Impact of sustained deprenyl (selegiline) in levodopa-treated Parkinson's disease: a randomized placebo-controlled extension of the deprenyl and tocopherol antioxidative therapy of parkinsonism trial. *Ann Neurol*. 2002;51:604–612.
65. Parkinson Study Group. A randomized placebo-controlled trial of rasagiline in levodopa-treated patients with Parkinson disease and motor fluctuations: the PRESTO study. *Arch Neurol*. 2005;62:241–248.
66. Amsterdam JD, Shults J. MAOI efficacy and safety in advanced stage treatment-resistant depression–a retrospective study. *J Affect Disord*. 2005;89:183–188.
67. Sheehan DV, Ballenger J, Jacobsen G. Treatment of endogenous anxiety with phobic, hysterical and hypochondriacal symptoms. *Arch Gen Psychiatry*. 1980;37:51–59.
68. Kaplan DR, Miller FD. Neurotrophin signal transduction in the nervous system. *Curr Opin Neurobiol*. 2000;10:381–391.
69. Nozaki K, Nishimura M, Hashimoto N. Mitogen-activated protein kinases and cerebral ischemia. *Mol Neurobiol*. 2001;23:1–19.
70. Hoefen RJ, Berk BC. The role of MAP kinases in endothelial activation. *Vascul Pharmacol*. 2002;38:271–273.
71. Liu Y, Shepherd EG, Nelin LD. MAPK phosphatases–regulating the immune response. *Nat Rev Immunol*. 2007;7:202–212.
72. Jiang SY, Zou YY, Wang JT. p38 mitogen-activated protein kinase-induced nuclear factor kappa-light-chain-enhancer of activated B cell activity is required for neuroprotection in retinal ischemia/reperfusion injury. *Mol Vis*. 2012;18:2096–2106.
73. Bachstetter AD, Van Eldik LJ. The p38 MAP kinase family as regulators of proinflammatory cytokine production in degenerative diseases of the CNS. *Aging Dis*. 2010;1:199–211.
74. Xing B, Bachstetter AD, Van Eldik LJ. Deficiency in p38beta MAPK fails to inhibit cytokine production or protect neurons against inflammatory insult in in vitro and in vivo mouse models. *PLoS One*. 2013;8:e56852.
75. Han D, Scott EL, Dong Y, Raz L, Wang R, Zhang Q. Attenuation of mitochondrial and nuclear p38alpha signaling: a novel mechanism of estrogen neuroprotection in cerebral ischemia. *Mol Cell Endocrinol*. 2015;400:21–31.
76. Xing B, Bachstetter AD, Van Eldik LJ. Inhibition of neuronal p38alpha, but not p38beta MAPK, provides neuroprotection against three different neurotoxic insults. *J Mol Neurosci*. 2015;55:509–518.
77. Kikuchi M, Tenneti L, Lipton SA. Role of p38 mitogen-activated protein kinase in axotomy-induced apoptosis of rat retinal ganglion cells. *J Neurosci*. 2000;20:5037–5044.
78. Katome T, Namekata K, Guo X, et al. Inhibition of ASK1-p38 pathway prevents neural cell death following optic nerve injury. *Cell Death Differ*. 2013;20:270–280.
79. Ferrari G, Terushkin V, Wolff MJ, et al. TGF-beta1 induces endothelial cell apoptosis by shifting VEGF activation of p38(MAPK) from the prosurvival p38beta to proapoptotic p38alpha. *Mol Cancer Res*. 2012;10:605–614.
80. Riederer P, Laux G. MAO-inhibitors in Parkinson's Disease. *Exp Neurobiol*. 2011;20:1–17.
81. Youdim MB, Weinstock M. Therapeutic applications of selective and non-selective inhibitors of monoamine oxidase A and B that do not cause significant tyramine potentiation. *Neurotoxicology*. 2004;25:243–250.

Investigative Ophthalmology & Visual Science